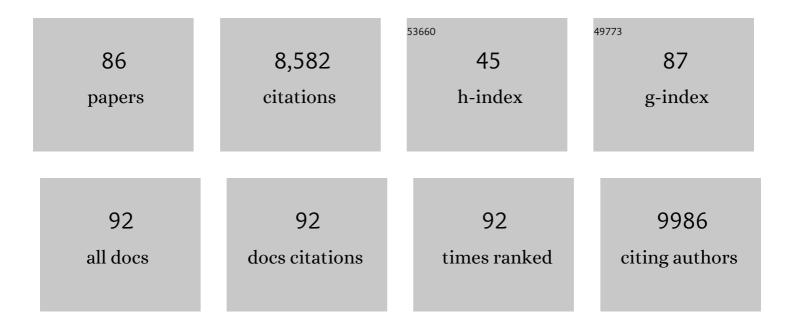
Seong-Min Bak

List of Publications by Year in descending order

Source: https://exaly.com/author-pdf/3174155/publications.pdf Version: 2024-02-01



#	Article	IF	CITATIONS
1	An ultrathin solid-state electrolyte film coated on LiNi0.8Co0.1Mn0.1O2 electrode surface for enhanced performance of lithium-ion batteries. Energy Storage Materials, 2022, 45, 1165-1174.	9.5	43
2	Surface Redox Pseudocapacitance of Partially Oxidized Titanium Carbide MXene in Water-in-Salt Electrolyte. ACS Energy Letters, 2022, 7, 30-35.	8.8	43
3	Hybrid MoS _{2+<i>x</i>} Nanosheet/Nanocarbon Heterostructures for Lithium-Ion Batteries. ACS Applied Nano Materials, 2022, 5, 5103-5118.	2.4	7
4	Investigation of Ca Insertion into α-MoO ₃ Nanoparticles for High Capacity Ca-Ion Cathodes. Nano Letters, 2022, 22, 2228-2235.	4.5	16
5	Isoxazole-Based Electrolytes for Lithium Metal Protection and Lithium-Sulfurized Polyacrylonitrile (SPAN) Battery Operating at Low Temperature. Journal of the Electrochemical Society, 2022, 169, 030513.	1.3	4
6	Carbon-free high-performance cathode for solid-state Li-O ₂ battery. Science Advances, 2022, 8, eabm8584.	4.7	15
7	The Role of Electron Localization in Covalency and Electrochemical Properties of Lithiumâ€lon Battery Cathode Materials. Advanced Functional Materials, 2021, 31, 2001633.	7.8	21
8	New Highâ€Performance Pbâ€Based Nanocomposite Anode Enabled by Wideâ€Range Pb Redox and Zintl Phase Transition. Advanced Functional Materials, 2021, 31, 2005362.	7.8	6
9	Identification of LiH and nanocrystalline LiF in the solid–electrolyte interphase of lithium metal anodes. Nature Nanotechnology, 2021, 16, 549-554.	15.6	171
10	<i>In Situ</i> ATRâ€FTIR Study of the Cathode–Electrolyte Interphase: Electrolyte Solution Structure, Transition Metal Redox, and Surface Layer Evolution. Batteries and Supercaps, 2021, 4, 778-784.	2.4	12
11	Tuning Sodium Occupancy Sites in P2â€Layered Cathode Material for Enhancing Electrochemical Performance. Advanced Energy Materials, 2021, 11, 2003455.	10.2	46
12	Hierarchical nickel valence gradient stabilizes high-nickel content layered cathode materials. Nature Communications, 2021, 12, 2350.	5.8	59
13	Modification of the Coordination Environment of Active Sites on MoC for Highâ€Efficiency CH ₄ Production. Advanced Energy Materials, 2021, 11, 2100044.	10.2	21
14	Understanding the Roles of the Electrode/Electrolyte Interface for Enabling Stable Liâ^¥Sulfurized Polyacrylonitrile Batteries. ACS Applied Materials & Interfaces, 2021, 13, 31733-31740.	4.0	25
15	Experimental Verification of Ir 5d Orbital States and Atomic Structures in Highly Active Amorphous Iridium Oxide Catalysts. ACS Catalysis, 2021, 11, 10084-10094.	5.5	4
16	Controlling MoO2 and MoO3 phases in MoOx/CNTs nanocomposites and their application to anode materials for lithium-ion batteries and capacitors. Electrochimica Acta, 2021, 388, 138635.	2.6	26
17	Reversible dual anionic-redox chemistry in NaCrSSe with fast charging capability. Journal of Power Sources, 2021, 502, 230022.	4.0	5
18	Sodium storage property and mechanism of NaCr1/4Fe1/4Ni1/4Ti1/4O2 cathode at various cut-off voltages. Energy Storage Materials, 2020, 24, 417-425.	9.5	25

#	Article	IF	CITATIONS
19	Structural Stabilization of P2â€ŧype Sodium Iron Manganese Oxides by Electrochemically Inactive Mg Substitution: Insights of Redox Behavior and Voltage Decay. ChemSusChem, 2020, 13, 5972-5982.	3.6	19
20	Biomimetic composite architecture achieves ultrahigh rate capability and cycling life of sodium ion battery cathodes. Applied Physics Reviews, 2020, 7, .	5.5	15
21	Mixed Ionic–Electronic Conductor of Perovskite Li <i>_x</i> La <i>_y</i> MO _{3â^} <i>_Î</i> toward Carbonâ€Free Cathode for Reversible Lithium–Air Batteries. Advanced Energy Materials, 2020, 10, 2001767.	10.2	32
22	Multimodal Analysis of Reaction Pathways of Cathode Materials for Lithium Ion Batteries. Microscopy and Microanalysis, 2020, 26, 906-908.	0.2	0
23	Reaction heterogeneity in practical high-energy lithium–sulfur pouch cells. Energy and Environmental Science, 2020, 13, 3620-3632.	15.6	127
24	A Co―and Niâ€Free P2/O3 Biphasic Lithium Stabilized Layered Oxide for Sodiumâ€Ion Batteries and its Cycling Behavior. Advanced Functional Materials, 2020, 30, 2003364.	7.8	80
25	Understanding the Mechanism of High Capacitance in Nickel Hexaaminobenzene-Based Conductive Metal–Organic Frameworks in Aqueous Electrolytes. ACS Nano, 2020, 14, 15919-15925.	7.3	46
26	Tailoring Solution-Processable Li Argyrodites Li _{6+<i>x</i>} P _{1–<i>x</i>} M _{<i>x</i>} S ₅ I (M = Ge, Sn) and Their Microstructural Evolution Revealed by Cryo-TEM for All-Solid-State Batteries. Nano Letters, 2020, 20, 4337-4345.	4.5	67
27	Revealing Reaction Pathways of Collective Substituted Iron Fluoride Electrode for Lithium Ion Batteries. ACS Nano, 2020, 14, 10276-10283.	7.3	14
28	Synchrotron Operando Depth Profiling Studies of State-of-Charge Gradients in Thick Li(Ni _{0.8} Mn _{0.1} Co _{0.1})O ₂ Cathode Films. Chemistry of Materials, 2020, 32, 6358-6364.	3.2	17
29	Anionic redox reaction in layered NaCr2/3Ti1/3S2 through electron holes formation and dimerization of S–S. Nature Communications, 2019, 10, 4458.	5.8	38
30	Improving the Electrochemical Performance and Structural Stability of the LiNi _{0.8} Co _{0.15} Al _{0.05} O ₂ Cathode Material at High-Voltage Charging through Ti Substitution. ACS Applied Materials & Interfaces, 2019, 11, 23213-23221.	4.0	57
31	Activating Layered Double Hydroxide with Multivacancies by Memory Effect for Energy-Efficient Hydrogen Production at Neutral pH. ACS Energy Letters, 2019, 4, 1412-1418.	8.8	115
32	Reversible Conversion Reactions and Small First Cycle Irreversible Capacity Loss in Metal Sulfideâ€Based Electrodes Enabled by Solid Electrolytes. Advanced Functional Materials, 2019, 29, 1901719.	7.8	21
33	Highâ€Voltage Chargingâ€Induced Strain, Heterogeneity, and Microâ€Cracks in Secondary Particles of a Nickelâ€Rich Layered Cathode Material. Advanced Functional Materials, 2019, 29, 1900247.	7.8	219
34	Anomalous metal segregation in lithium-rich material provides design rules for stable cathode in lithium-ion battery. Nature Communications, 2019, 10, 1650.	5.8	60
35	Synthesis and Characterization of a Molecularly Designed Highâ€Performance Organodisulfide as Cathode Material for Lithium Batteries. Advanced Energy Materials, 2019, 9, 1900705.	10.2	34
36	Optimizing PtFe intermetallics for oxygen reduction reaction: from DFT screening to <i>in situ</i> XAFS characterization. Nanoscale, 2019, 11, 20301-20306.	2.8	33

#	Article	IF	CITATIONS
37	Rational Design of Hierarchically Openâ€Porous Spherical Hybrid Architectures for Lithiumâ€Ion Batteries. Advanced Energy Materials, 2019, 9, 1802816.	10.2	48
38	Innenrücktitelbild: Atomically Dispersed Molybdenum Catalysts for Efficient Ambient Nitrogen Fixation (Angew. Chem. 8/2019). Angewandte Chemie, 2019, 131, 2547-2547.	1.6	7
39	Atomically Dispersed Molybdenum Catalysts for Efficient Ambient Nitrogen Fixation. Angewandte Chemie - International Edition, 2019, 58, 2321-2325.	7.2	543
40	Atomically Dispersed Molybdenum Catalysts for Efficient Ambient Nitrogen Fixation. Angewandte Chemie, 2019, 131, 2343-2347.	1.6	95
41	Confinement of Ultrasmall Cobalt Oxide Clusters within Silicalite-1 Crystals for Efficient Conversion of Fructose into Methyl Lactate. ACS Catalysis, 2019, 9, 1923-1930.	5.5	39
42	Native Vacancy Enhanced Oxygen Redox Reversibility and Structural Robustness. Advanced Energy Materials, 2019, 9, 1803087.	10.2	70
43	Advanced Characterization Techniques for Sodiumâ€ion Battery Studies. Advanced Energy Materials, 2018, 8, 1702588.	10.2	122
44	In situ/operando synchrotron-based X-ray techniques for lithium-ion battery research. NPG Asia Materials, 2018, 10, 563-580.	3.8	261
45	Evolution of redox couples in Li- and Mn-rich cathode materials and mitigation of voltage fade by reducing oxygen release. Nature Energy, 2018, 3, 690-698.	19.8	675
46	Introducing Fe ²⁺ into Nickel–Iron Layered Double Hydroxide: Local Structure Modulated Water Oxidation Activity. Angewandte Chemie, 2018, 130, 9536-9540.	1.6	86
47	Introducing Fe ²⁺ into Nickel–Iron Layered Double Hydroxide: Local Structure Modulated Water Oxidation Activity. Angewandte Chemie - International Edition, 2018, 57, 9392-9396.	7.2	284
48	High energy-density and reversibility of iron fluoride cathode enabled via an intercalation-extrusion reaction. Nature Communications, 2018, 9, 2324.	5.8	136
49	Investigation of Degradation Pathway in High Ni-Content Cathode Materials at Primary and Secondary Particle Level By Multi-Scale Characterization. ECS Meeting Abstracts, 2018, , .	0.0	0
50	Suppressing the chromium disproportionation reaction in O3-type layered cathode materials for high capacity sodium-ion batteries. Journal of Materials Chemistry A, 2017, 5, 5442-5448.	5.2	45
51	Electronic structural studies on the improved thermal stability of Li(Ni0.8Co0.15Al0.05)O2 by ZrO2 coating for lithium ion batteries. Journal of Applied Electrochemistry, 2017, 47, 565-572.	1.5	9
52	Self-assembled Li3V2(PO4)3/reduced graphene oxide multilayer composite prepared by sequential adsorption. Journal of Power Sources, 2017, 367, 167-176.	4.0	5
53	Utilizing Co ²⁺ /Co ³⁺ Redox Couple in P2‣ayered Na _{0.66} Co _{0.22} Mn _{0.44} Ti _{0.34} O ₂ Cathode for Sodium″on Batteries. Advanced Science, 2017, 4, 1700219.	5.6	85
54	Naâ€ion Intercalation and Charge Storage Mechanism in 2D Vanadium Carbide. Advanced Energy Materials, 2017, 7, 1700959.	10.2	168

#	Article	IF	CITATIONS
55	Strategies to curb structural changes of lithium/transition metal oxide cathode materials & the changes' effects on thermal & cycling stability. Chinese Physics B, 2016, 25, 018205.	0.7	13
56	Explore the Effects of Microstructural Defects on Voltage Fade of Li- and Mn-Rich Cathodes. Nano Letters, 2016, 16, 5999-6007.	4.5	64
57	Highâ€Rate Charging Induced Intermediate Phases and Structural Changes of Layerâ€Structured Cathode for Lithiumâ€lon Batteries. Advanced Energy Materials, 2016, 6, 1600597.	10.2	110
58	Quantification of Honeycomb Number-Type Stacking Faults: Application to Na ₃ Ni ₂ BiO ₆ Cathodes for Na-Ion Batteries. Inorganic Chemistry, 2016, 55, 8478-8492.	1.9	51
59	Utilizing Environmental Friendly Iron as a Substitution Element in Spinel Structured Cathode Materials for Safer High Energy Lithiumâ€lon Batteries. Advanced Energy Materials, 2016, 6, 1501662.	10.2	35
60	Scalable fabrication of micron-scale graphene nanomeshes for high-performance supercapacitor applications. Energy and Environmental Science, 2016, 9, 1270-1281.	15.6	122
61	Probing the Mechanism of High Capacitance in 2D Titanium Carbide Using In Situ Xâ€Ray Absorption Spectroscopy. Advanced Energy Materials, 2015, 5, 1500589.	10.2	521
62	Highâ€Surfaceâ€Area Nitrogenâ€Doped Reduced Graphene Oxide for Electric Double‣ayer Capacitors. ChemSusChem, 2015, 8, 1875-1884.	3.6	83
63	Unveiling Surface Redox Charge Storage of Interacting Two-Dimensional Heteronanosheets in Hierarchical Architectures. Nano Letters, 2015, 15, 2269-2277.	4.5	80
64	Using Real-Time Electron Microscopy To Explore the Effects of Transition-Metal Composition on the Local Thermal Stability in Charged Li _{<i>x</i>} Ni _{<i>y</i>} Mn _{<i>z</i>} Co _{1–<i>y</i>–<i>z</i>} O Cathode Materials. Chemistry of Materials, 2015, 27, 3927-3935.	_{2<!--</td--><td>sub></td>}	sub>
65	Direct Observation of the Redistribution of Sulfur and Polysufides in Li–S Batteries During the First Cycle by In Situ Xâ€Ray Fluorescence Microscopy. Advanced Energy Materials, 2015, 5, 1500072.	10.2	84
66	O3-type layered transition metal oxide Na(NiCoFeTi) _{1/4} O ₂ as a high rate and long cycle life cathode material for sodium ion batteries. Journal of Materials Chemistry A, 2015, 3, 23261-23267.	5.2	95
67	Investigating the Reversibility of Structural Modifications of Li _{<i>x</i>} Ni _{<i>y</i>} Mn _{<i>z</i>} Co _{1–<i>y</i>–<i>z</i>} O Cathode Materials during Initial Charge/Discharge, at Multiple Length Scales. Chemistry of Materials, 2015. 27. 6044-6052.	_{2<!--</td--><td>sub> 80</td>}	sub> 80
68	Thermal stability in the blended lithium manganese oxide – Lithium nickel cobalt manganese oxide cathode materials: An in situ time-resolved X-Ray diffraction and mass spectroscopy study. Journal of Power Sources, 2015, 277, 193-197.	4.0	33
69	One-step preparation of reduced graphene oxide/carbon nanotube hybrid thin film by electrostatic spray deposition for supercapacitor applications. Metals and Materials International, 2014, 20, 975-981.	1.8	16
70	Structural Changes and Thermal Stability of Charged LiNi _{<i>x</i>} Mn _{<i>y</i>} Co _{<i>z</i>} O ₂ Cathode Materials Studied by Combined <i>In Situ</i> Time-Resolved XRD and Mass Spectroscopy. ACS Applied Materials & Interfaces, 2014, 6, 22594-22601.	4.0	731
71	Structural Changes in Reduced Graphene Oxide upon MnO ₂ Deposition by the Redox Reaction between Carbon and Permanganate Ions. Journal of Physical Chemistry C, 2014, 118, 2834-2843.	1.5	57
72	Improved high-voltage performance of FePO4-coated LiCoO2 by microwave-assisted hydrothermal method. Electrochemistry Communications, 2014, 43, 113-116.	2.3	34

#	Article	IF	CITATIONS
73	Understanding the Rate Capability of Highâ€Energyâ€Density Liâ€Rich Layered Li _{1.2} Ni _{0.15} Co _{0.1} Mn _{0.55} O ₂ Cathode Materials. Advanced Energy Materials, 2014, 4, 1300950.	10.2	480
74	Oxygen-Release-Related Thermal Stability and Decomposition Pathways of Li _{<i>x</i>} Ni _{0.5} Mn _{1.5} O ₄ Cathode Materials. Chemistry of Materials, 2014, 26, 1108-1118.	3.2	75
75	Investigating Local Degradation and Thermal Stability of Charged Nickel-Based Cathode Materials through Real-Time Electron Microscopy. ACS Applied Materials & Interfaces, 2014, 6, 15140-15147.	4.0	90
76	SYNTHESIS OF HYDROUS RUTHENIUM OXIDE NANOPARTICLES IN SUB- AND SUPERCRITICAL WATER AND THEIR CAPACITIVE PROPERTIES. Chemical Engineering Communications, 2014, 201, 1259-1269.	1.5	2
77	Soft templated mesoporous manganese oxide/carbon nanotube composites via interfacial surfactant assembly. Journal of Materials Chemistry A, 2014, 2, 3641-3647.	5.2	15
78	Combining In Situ Synchrotron Xâ€Ray Diffraction and Absorption Techniques with Transmission Electron Microscopy to Study the Origin of Thermal Instability in Overcharged Cathode Materials for Lithiumâ€Ion Batteries. Advanced Functional Materials, 2013, 23, 1047-1063.	7.8	458
79	Correlating Structural Changes and Gas Evolution during the Thermal Decomposition of Charged Li _{<i>x</i>} Ni _{0.8} Co _{0.15} Al _{0.05} O ₂ Cathode Materials. Chemistry of Materials, 2013, 25, 337-351.	3.2	317
80	Phase transition behavior of NaCrO2 during sodium extraction studied by synchrotron-based X-ray diffraction and absorption spectroscopy. Journal of Materials Chemistry A, 2013, 1, 11130.	5.2	84
81	Cathode Materials: Combining In Situ Synchrotron Xâ€Ray Diffraction and Absorption Techniques with Transmission Electron Microscopy to Study the Origin of Thermal Instability in Overcharged Cathode Materials for Lithiumâ€Ion Batteries (Adv. Funct. Mater. 8/2013). Advanced Functional Materials, 2013, 23, 1046-1046.	7.8	7
82	Mesoporous nickel/carbon nanotube hybrid material prepared by electroless deposition. Journal of Materials Chemistry, 2011, 21, 1984-1990.	6.7	61
83	Spinel LiMn2O4/reduced graphene oxide hybrid for high rate lithium ion batteries. Journal of Materials Chemistry, 2011, 21, 17309.	6.7	138
84	Solid-state microwave irradiation synthesis of high quality graphenenanosheets under hydrogen containing atmosphere. Journal of Materials Chemistry, 2011, 21, 680-686.	6.7	138
85	Li4Ti5O12/reduced graphite oxide nano-hybrid material for high rate lithium-ion batteries. Electrochemistry Communications, 2010, 12, 1768-1771.	2.3	114
86	Nano-sized lithium manganese oxide dispersed on carbon nanotubes for energy storage applications. Electrochemistry Communications, 2009, 11, 1575-1578.	2.3	57